Volume 1 | Number 1 | Jan 2013 | Pages 1–100

Polymer Chemistry

www.rsc.org/polymers

ROYAL SOCIETY OF CHEMISTRY

ROYAL SOCIETY OF CHEMISTRY

www.rsc.org/polymers

Polymer Chemistry

Polymer Chemistry

ARTICLE TYPE

Synthesis of Well-defined Functionalized Poly(2-(Diisopropylamino)ethyl Methacrylate) Using ATRP with Sodium Dithionite as a SARA Agent

Joana R. Góis,[a] Nuno Rocha,[a] Anatoliy V. Popov,[b] Tamaz Guliashvili,[c] Krzysztof Matyjaszewski,[d]
5 **Arménio C. Serra,[a] Jorge F. J. Coelho[a]***

2-(Diisopropylamino)ethyl methacrylate (DPA) was polymerized by Atom Transfer Radical
10 Polymerization (ATRP) using sodium dithionite ($Na_2S_2O_4$) as a reducing agent and supplemental
activator with $Cu(II)Br_2/Me_6TREN$ catalytic system at 40 °C in a mixture isopropanol-water. The effects
of the solvent mixture and the initiator structure on the polymerization kinetics were studied. The eco-
friendly catalytic system described is suitable for the synthesis poly(2-(diisopropylamino)ethyl
methacrylate) (PDPA) with controlled molecular weight, low dispersity, and well-defined chain-end
15 functionality. Both linear and 4-arms star polymers with various target molecular weights were
synthesised. The ^{1}H NMR and MALDI-TOF analysis confirmed the molecular structure and high chain-
end functionality of the obtained polymers. The use of an alkyne functionalized initiator allowed further
azide-alkyne Huisgen cycloaddition with 3-azido-7-diethylaminocoumarin, a fluorescent biocompatible
molecule.

20 The discovery of controlled/"living" radical polymerization (CLRP) methods has brought an unprecedented interest over this technology during the last two decades.[1] The possibility of synthesizing tailor made polymers with controlled composition, architecture, molecular weight (MW) and active chain-end 25 functionalities by radical reactions opened a myriad of opportunities for macromolecular engineering. Among several CLRP methods reported in the literature, ATRP is the most often used due to several intrinsic advantages, such as simplicity, high tolerance to different monomer functionalities, and the 30 commercial availability of most compounds. In order to reduce the catalyst levels, several variations of the initial ATRP concept have been reported in the literature, such as activators regenerated by electron transfer (ARGET) ATRP,[2] initiator for continuous activator regeneration (ICAR) ATRP,[3] supplemental activator 35 and reducing agent (SARA) ATRP,[4, 5] and polymerization in the presence of Cu^0.[6-9] These methods require ppm amounts of the catalyst to afford fast and controlled polymerization at room temperature. Organic sulphites have recently been reported by our research group as very efficient SARA agents).[10, 11] Amongst 40 the organic sulphites that were studied, sodium dithionite $(Na_2S_2O_4)$[12] is the most efficient reducing agent that can reduce the Cu(II) species into Cu(I).[10, 11] The reactions proceeded in a very controlled manner in alcohol/water solvent mixtures, with faster polymerization at higher contents of water in the system.[11]

45 Poly(2-(diisopropylamino)ethyl methacrylate) (PDPA) is a tertiary amine methacrylate with a hydrophilic/hydrophobic transition at pH around 6.2,[13, 14] making it a very attractive polymer for biomedical applications. Several studies have been reported using DPA-based copolymers for the preparation of 50 smart vesicles[15, 16] and micelles[17] for gene and drug delivery applications.[14, 18] The first report concerning the ATRP of DPA was carried out in methanol with a Cu(I)Br/2,2'-bipyridine (Bpy) complex using an water soluble poly(2-methacryloyloxyethyl phosphorylcholine) macroinitiator.[19] Thereafter, several DPA 55 based copolymers were synthesized using the same approach with slightly variations in the solvent used and the copper based catalytic complexes: Cu(I)Br/1,1,4,7,10,10-hexamethyltri-ethylenetetramine (HMTETA) ;[20] Cu(I)Br/ *N,N,N',N'',N''*-penta-methyldiethylenetriamine (PMDETA);[18] or Cu(I)Cl/PMDETA,[21] 60 and Cu(I)Cl/Bpy.[22] The aforementioned systems required a considerable amount of catalyst to control the polymerization and to afford polymers of low dispersity. This fact is a serious issue if one intends to prepare well-controlled PDPA molecular structures for biomedical applications, requiring, for instance, highly 65 demanding purification procedures.[23]

Concerning the potential of PDPA-based polymeric structures for biomedical applications,[18, 21, 24] hereafter it is proposed the ATRP of DPA using a more biocompatible and eco-friendly catalyst system that involves the use of FDA approved additives in the 70 presence of only trace amounts of copper. The influence of the

solvent and the ATRP initiator were evaluated in the SARA ATRP of DPA using $Na_2S_2O_4$ as a reducing agent (and supplemental activator). The use of alkyne-terminated initiators allowed a further conjugation of the products with other molecules or polymers by a "click" reaction with no need of any post-modification reactions. The 3-azido-7-diethylamino-coumarin molecule was used as a model azido-compound, since the formation of a fluorescent product can confirm the success of the "click" reaction.[25] The living character of the synthesised PDPA also allowed the polymeric chain-growth to obtain copolymeric structures or any post-polymerization modification. Moreover, the combination with the biocompatible coumarin dye can be used to provide fluorescent molecular probing to these materials.[25, 26]

Experimental

Materials

2-(Diisopropylamino)ethyl methacrylate (Aldrich, 97% stabilized), was passed over a sand/alumina column before use in order to remove the hydroquinone inhibitors. Sodium dithionite ($Na_2S_2O_4$) (Merck, >87%), copper(II) bromide ($CuBr_2$) (Acros, 99+%+ extra pure, anhydrous), copper(II) sulphate ($CuSO_4$) (Sigma, , ≥99%), sodium ascorbate (Sigma, ≥98%), ethyl 2-bromoisobutyrate (EBiB) (98%; Aldrich), pentaerythritol tetrakis(2-bromoisobutyrate) (4f-BiB) (97%; Aldrich), deuterated chloroform ($CDCl_3$) (Euriso-top, +1% TMS), 2-propanol (IPA) (Fisher Chemical), tetrahydrofuran (THF) (Fisher Chemical), poly(ethylene glycol) (PEG) standards (Fluka, analytical standards for GPC), were used as received. Me_6TREN and propargyl 2-bromoisobutyrate (PgBiB) were synthesized according the procedures described in the literature[27, 28] (PgBiB: ^{1}H NMR (400 MHz, $CDCl_3$, δ): 4.90 (2H, COOCH); 4.90 (2H, $COOCH_2$); 2.50 (1H, $COOCH_2≡CH$); 1.80 (6H, $C(CH_3)_2$). 3-azido-7-diethylaminocoumarin (N_3-Cum) was synthesized according to the procedures described in the literature [25] (^{1}H NMR (400 MHz, $CDCl_3$, δ): 7.21 (d, 2H); 7.11 (s, 1H); 6.57 (s, 1H); 3.46 (q, 4H); 1.21 (t, 6H). Purified water (Milli-Q®, Millipore, resistivity >18 MΩ cm) was obtained by reverse osmosis.

Techniques

Size exclusion chromatography (SEC) analysis was performed using a system equipped with an online degasser, a refractive index (RI) detector and a set of columns: Shodex OHpak SB-G guard column, OHpak SB-802.5HQ and OHpak SB-804HQ columns. The polymers were eluted at a flow rate of 0.5 mL/min with 0.1 M Na_2SO_4 (aq)/1 wt% acetic acid/0.02% NaN_3 at 40 ºC. Before the injection (50 µL) the samples were filtered through a polyester membrane with 0.45µm pore. The system was calibrated with narrow dispersity PEG standards. The number-average molecular weight ($M_{n,GPC}$) and dispersity, (Đ) (M_w/M_n) of the synthesised polymers were determined by conventional calibration using Clarity software version 2.8.2.648.

For the 4-armed polymers, high performance gel permeation chromatography (HPSEC) was performed using a Viscotek (ViscotekTDAmax) with a differential viscometer (DV), right-angle laser-light scattering (RALLS, Viscotek), and refractive index (RI) detectors, using column set of a PL 10 µm guard column followed by one MIXED-E PLgel column and one MIXED-C PLgel column. Previously filtered THF was used as an eluent at a flow rate of 1 mL/min at 30 ºC. The samples were filtered through a polytetrafluoroethylene membrane with 0.2 µm pore before injection and the system was calibrated with narrow PS standards. The *dn/dc* of PDPA in THF at 30 °C was determined as 0.077 using a RUDOLPH RESEARCH J357 Automatic Refractometer (J357-NDS-670-CC), $M_{n,GPC}$ and Đ of synthesized polymers were determined by using a multidetectors calibration (OmniSEC software version: 4.6.1.354).

[1]H nuclear magnetic resonance (NMR) spectra were recorded on a Bruker Avance III 400 MHz spectrometer, with a 5 mm TXI triple resonance detection probe, in $CDCl_3$ with tetramethylsilane (TMS) as an internal standard. Conversion of monomers was determined by integration of monomer and polymer peaks using MestReNova software version: 6.0.2-5475.

For matrix-assisted laser desorption ionization time-of-flight mass spectroscopy (MALDITOF-MS) analysis, the PDPA samples were dissolved in THF at a concentration of 20 mg/mL and 2,5-dihydroxybenzoic acid (DHB) (20 mg/mL in THF) was used as a matrix. The dried-droplet sample preparation technique was used to obtain a 1:1 ratio (sample/matrix); an aliquot of 1 µL of each sample was directly spotted on the MTP AnchorChip TM 600/384 TF MALDI target, BrukerDaltonik (Bremen Germany) and, before the sample dried, 1 µL of matrix solution in THF was added and the mixture allowed to dry at room temperature, to allow matrix crystallization. External mass calibration was performed with a peptide calibration standard (PSCII) for the range 700-3000 (9 mass calibration points), 0.5 µL of the calibration solution and matrix previously mixed in an Eppendorf tube (1:2, v/v) were applied directly on the target and allowed to dry at room temperature. Mass spectra were recorded using an Autoflex III smartbeam1 MALDITOF-MS mass spectrometer Bruker Daltonik (Bremen, Germany) operating in the linear and reflection positive ion mode. Ions were formed upon irradiation by a smart beam laser using a frequency of 200 Hz. Each mass spectrum was produced by averaging 2500 laser shots collected across the whole sample spot surface by screening in the range m/z 500-7500. The laser irradiance was set to 35-40 % (relative scale 0-100) arbitrary units according to the corresponding threshold required for the applied matrix systems.

Procedures

Typical procedure for the SARA ATRP of DPA (DP = 50) catalyzed by [$Na_2S_2O_4$]/[$CuBr_2$]/[Me_6TREN] = 1/0.1/0.1 in isopropanol/water mixture. A mixture of $CuBr_2$ (3.67 mg, 0.016 mmol), Me_6TREN (4.16 mg, 0.018 mmol) and water (195 µL) was placed in a Schlenk tube reactor that was sealed by using a rubber septa. $Na_2S_2O_4$ (32.86 mg, 0.164 mmol) and a mixture of DPA (1.75 g, 8.21 mmol) and EBiB (32.02 mg, 0.164 mmol) in IPA (3.697 mL) (previously bubbled with nitrogen for about 15 minutes) was added to the reactor and frozen in liquid nitrogen. The Schlenk tube reactor containing the reaction mixture was

deoxygenated with three freeze-vacuum-thaw cycles and purged with nitrogen. The Schlenk tube reactor was placed in a water bath at 40 ºC with stirring (600 rpm). Aliquots of the reaction mixture were collected periodically during the polymerization by
5 using an airtight syringe and purging the side arm of the Schlenk tube reactor with nitrogen. The samples were analyzed by ^{1}H NMR spectroscopy in order to determine the monomer conversion, and by SEC to determine MW and $Đ$ of the PDPA.

Chain extension experiment. A mixture of $CuBr_2$ (4.84mg,
10 0.02 mmol), Me_6TREN (5.48 mg, 0.02 mmol) and water (152 µL) was placed in a Schlenk tube reactor that was sealed by using rubber septa. $Na_2S_2O_4$ (47.5 mg, 0.0.24 mmol) and a mixture of DPA (1.37 g, 6.42 mmol) and EBiB (41.7 mg, 0.21 mmol) in IPA (2.892 mL) (previously bubbled with nitrogen for about 15
15 minutes) was added to the reactor and frozen in liquid nitrogen. The Schlenk tube reactor containing the reaction mixture was deoxygenated with five freeze-vacuum thaw cycles and purged with nitrogen. The Schlenk tube reactor was placed in a water bath at 40 ºC with stirring (600 rpm) and the reaction proceeded
20 for 4 hours (75% conversion, $M_{n,th}$= 4940 gmol^{-1}, $M_{n, GPC}$= 15300 gmol^{-1}, M_w/M_n = 1.20). After that, a degased solution of DPA (1.61g, 7.56 mmol) in IPA/H_2O (2.76 mL/145 µL) was added and the reaction proceeded for 24h.

**"Click" reaction between the alkyne terminated-PDPA
25 (AT-PDPA) and 3-azido-7-diethylamino coumarin (N_3-Cum).** AT-PDPA (341.16 mg, 0.012 mmol, $M_{n, GPC}$ = 27600 gmol^{-1}, M_w/M_n = 1.11) synthesized by SARA ATRP and N_3-Cum (4.81 mg, 0.018 mmol)) were dissolved in 6 mL of THF. Sodium ascorbate (1.96 mg, 0.010 mmol dissolved in water (0.4 mL)
30 were added to the previous mixture, the vessel were sealed with a rubber septum and the mixture bubbled with Nitrogen for about 10 min. A fresh solution of $CuSO_4$ (0.54 mL, 0.003 mmol) in water were added under N_2 and the reaction proceed at room temperature overnight. The reaction was observed by UV
35 fluorescence at 366 nm. To remove the excess of N_3-Cum and the catalysts, the product was dialysed against THF-water mixture (50:50) for 2 days. The product was analysed by NMR and by fluorescence restoration (λ_{ex}= 365 nm) in order to confirm the success of the "click" reaction.

40 **Results and discussion**

The reports available in the literature concerning the ATRP of DPA based polymers involve the use of high concentration of copper catalysts and, in some cases toxic solvents, such as THF or methanol. The control over the polymerization is achieved by
45 Cu(I)Br (or Cu(I)Cl) chelated with various nitrogen based ligands such as Bpy,[13, 19, 22, 29] PMDETA[21] or HMTETA[20] at high concentrations. However, polymers intended to be applied in the biomedical field requires the use of safer solvent mixtures and an accurate removal of the catalyst from the final product.
50 The use of inorganic sulfites, such as $Na_2S_2O_5$, $Na_2S_2O_4$ and $NaHSO_3$, as reducing agents and supplemental activators in ATRP of methyl acrylate (MA) has recently been reported.[10, 11] The ability to control the polymerization with small amounts of
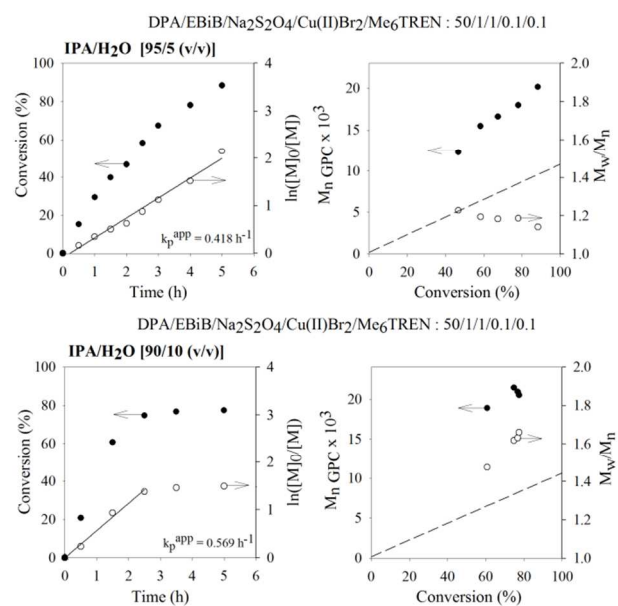

55 **Fig. 1** Kinetic plots of DPA conversion and ln[M]$_0$/[M] vs time and plot of number average molecular weights ($M_{n,GPC}$) and dispersity (M_w/M_n) vs conversion for ATRP of DPA in the presence of Cu(II)Br$_2$/Me$_6$TREN with $Na_2S_2O_4$ in two different IPA/water mixtures. Conditions: [DPA]$_0$/solvent = 1/2 (v/v), [IPA]/[H_2O] = 0.95/0.05 (v/v) or 0.90/0.10
60 (v/v); [DPA]$_0$ /[EBiB]$_0$ /[$Na_2S_2O_4$]$_0$ /[CuBr$_2$]$_0$ /[Me$_6$TREN]$_0$ = 50/1/1/0.1/0.1 (molar); T= 40 °C.

copper/ligand system in alcohol/water mixture makes these systems very promising for polymer synthesis for biomedical
65 applications.
As the amount of water has a strong impact on the kinetics of ATRP, initially, the experiments were conducted to determine influence of water content in the SARA ATRP of DPA using $Na_2S_2O_4$ as a reducing agent.[11] Subsequently, the method was
70 applied for the polymerization of DPA with various target molecular weights and different ATRP initiators (alkyne terminated initiator (PgBiB) and a 4-arms star initiator). All reactions were performed using a ratio [DPA]$_0$/solvent = 1/2 (v/v) and a molar ratio [$Na_2S_2O_4$]$_0$/[CuBr$_2$]$_0$/[Me$_6$TREN]$_0$=1/0.1/0.1.

75 **Influence of water content on the rate of polymerization and control over molar mass of DPA in IPA/water mixtures**
In SARA ATRP mediated by a mixed sulfite-Cu(II)Br$_2$/ligand catalytic system the use of small amounts of water in the reaction mixture can enhance the solubilization of the inorganic salts
80 leading to faster reactions. [11] Abreu and co-authors have found that for the system [methyl acrylate]$_0$/[EBiB]$_0$/[$Na_2S_2O_4$]$_0$/ [Cu(II)Br$_2$]$_0$/[Me$_6$TREN]$_0$ polymerization of methyl acrylate in a mixture ethanol/water, the optimum content of water was 35%. Up to this value, the polymerization rate increased with the water
85 content maintaining the control over the MW and dispersity.[11]
In order to find the optimal ratio of IPA/water to afford a controlled ATRP of DPA, two different ratios IPA/water have been studied. Fig.1 presents the kinetic plots of SARA ATRP of

DPA conducted at 40 °C in IPA/water mixtures using 5 or 10% (v/v) of water in the solvent mixture.
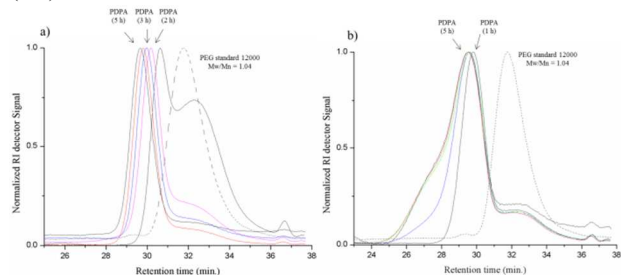

Fig. 2 GPC traces of PEG standard (M_p = 12 000 gmol^{-1}; Mw/Mn = 1.04)
5 and PDPA samples. Conditions: (a) [DPA]$_0$/solvent = 1/2 (v/v), [IPA]/[H$_2$O] = 0.95/0.05 (v/v); [DPA]$_0$ /[EBiB]$_0$ /[Na$_2$S$_2$O$_4$]$_0$ /[CuBr$_2$]$_0$ /[Me$_6$TREN]$_0$ = 50/1/1/0.1/0.1 (molar); T= 40ºC; (b) [DPA]$_0$/solvent = 1/2 (v/v), [IPA]/[H$_2$O] = 0.90/0.10 (v/v), [DPA]$_0$ /[EBiB]$_0$ /[Na$_2$S$_2$O$_4$]$_0$ /[CuBr$_2$]$_0$ /[Me$_6$TREN]$_0$ = 50/1/1 /0.1/0.1 (molar); T= 40.

10

It should be mentioned that to poor solubility of sodium dithionite in isopropanol, the polymerizations should always be carried out in the presence of small amount of water. The presence of 5% (v/v) of water in the reaction solvent mixture allows the
15 polymerization to proceed with a first order kinetic relative to the monomer, reaching 80% conversion in 5 hours, with low dispersity values (M_w/M_n = 1.14). The SEC traces (Fig. 2(a)) of the samples that were taken at different reaction times show that, for the polymerization carried out at 5% (v/v) of water, a
20 unimodal distribution and a gradual shift towards higher MW with time was obtained. When the ATRP was conducted with a high water content, (10%, v/v) in the solvent mixture, a lower monomer conversion and an uncontrolled polymerization was observed. This fact is supported by the deviations of the ATRP
25 kinetics from a "living" behavior[30] in Fig. 1 and by broad GPC traces that are shown in Fig.2(b). The high dispersity may result from the reduced solubility of PDPA in this solvent mixture (IPA/H$_2$O = 90/10 (v/v)). In fact, it has been experimentally observed that for 10 % (v/v) of water, the synthesized PDPA
30 samples of higher MW presented significantly lower solubility in the solvent mixture when compared to those with 5% (v/v) of water. Although most of the critical characteristics of a "living" polymerization are achieved, such as the linear growth of molecular weight with conversion and low dispersity values
35 throughout the reaction, when ATRP was carried with 5%(v/v) of water , the GPC traces present a tailing in the GPC curve. This deviation become less predominant for higher DPA monomer conversion, suggesting the occurrence of termination reactions at the early stages of the polymerization due to the high
40 concentration of radicals caused by the presence of the dithionite.[12, 31, 32]

Study of variable degrees of polymerization
The influence of the target DP on the SARA ATRP of DPA is presented in Fig. 3. As expected, the polymerization rate
45 decreases for a higher targeted DP. This decrease can be attributed to a lower concentration of radicals in the polymerization mixture. Although the kinetics of polymerization

at DP 100 shows a typical profile of a "living" polymerization, with a linear increase of the MW with the conversion, there is a
50 tendency towards higher dispersities when compared to those obtained at the DP of 50. Fig.4 compares the GPC traces obtained for DP=100 and 20.
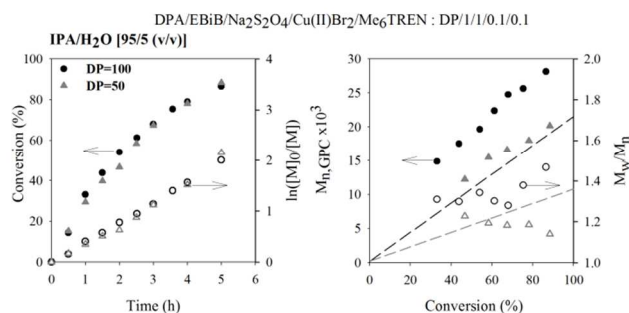

55 **Fig. 3** Kinetic plots of DPA conversion and ln[M]$_0$/[M] vs time and plot of number average MW ($M_{n,GPC}$) and dispersity (M_w/M_n) vs conversion for ATRP of DPA in the presence of Cu(II)Br$_2$/Me$_6$TREN with Na$_2$S$_2$O$_4$ for two different DP, 100 and 50. Conditions: [DPA]$_0$/solvent = 1/2 (v/v), [IPA]/[H$_2$O] = 0.95/0.05 (v/v); [DPA]$_0$ /[EBiB]$_0$ /[Na$_2$S$_2$O$_4$]$_0$ /[CuBr$_2$]$_0$
60 /[Me$_6$TREN]$_0$ = 100/1/1/0.1/0.1 (molar) T= 40ºC.

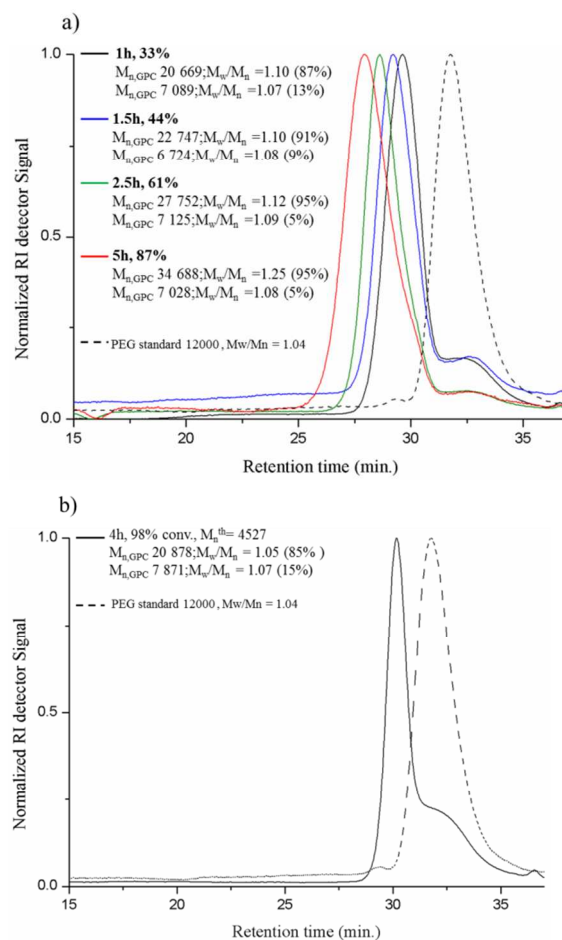**Fig. 4** GPC traces of PEG standard (Mp = 12 000 gmol^{-1}; Mw/Mn = 1.04) and PDPA samples for two different target MW (DP 100 (a) and DP 20
65 (b)). Conditions: [DPA]$_0$/solvent = 1/2 (v/v), [IPA]/[H$_2$O] = 0.95/0.05 (v/v); (a): [DPA]$_0$ /[EBiB]$_0$ /[Na$_2$S$_2$O$_4$]$_0$ /[CuBr$_2$]$_0$ /[Me$_6$TREN]$_0$ =

100/1/1/0.1/0.1 (molar); (b): [DPA]$_0$ /[EBiB]$_0$ /[Na$_2$S$_2$O$_4$]$_0$ /[CuBr$_2$]$_0$ /[Me$_6$TREN]$_0$ = 20/1/1/0.1/0.1 (molar); T= 40ºC.

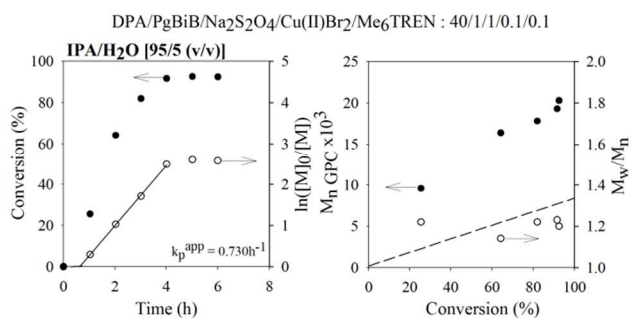DPA/PgBiB/Na$_2$S$_2$O$_4$/Cu(II)Br$_2$/Me$_6$TREN : 40/1/1/0.1/0.1

Fig. 5 Kinetic plots of DPA conversion and ln[M]$_0$/[M] vs time and plot of number average MW (M$_{n,GPC}$) and dispersity (M$_w$/M$_n$) vs conversion for ATRP of DPA in the presence of Cu(II)Br$_2$/Me$_6$TREN with Na$_2$S$_2$O$_4$. Conditions: [DPA]$_0$/solvent = 1/2 (v/v), [IPA]/[H$_2$O] = 0.95/0.05 (v/v); [DPA]$_0$ /[PgBiB]$_0$ /[Na$_2$S$_2$O$_4$]$_0$ /[CuBr$_2$]$_0$ /[Me$_6$TREN]$_0$ = 40/1/1/0.1/0.1 (molar) T= 40ºC.

The GPC traces obtained for DP of 100 shows a shift towards higher MW values with time, but, in this case, the tailing for lower MW segments is not as evident as for lower DP. This observation may be attributed to a lower concentration of dead chain ends, likely due to the reduced concentration of radicals. In fact, polymerizations with a much lower DP (20) (Fig.4(b)) show GPC curves with more evident low MW tail. For the other polymerizations carried out with higher DP, the main peak remains with a narrow distribution, still suggesting a controlled PDPA chain growth. The formation of lower MW fraction which decreases with the monomer conversion, suggests that there is a loss of active chain end functionality at the beginning of the polymerization. This effect may be attributed to the high concentration of sodium dithionite and possible inefficient deactivation by the Cu(II)Br$_2$ complex, leading to termination reactions and becoming more pronounced when the catalyst is at a higher concentration.

To further evaluate the effect of the Cu(II)Br$_2$/Me$_6$TREN complex concentration in the formation of these low MW PDPA fractions, two similar reactions were performed using different ratios of the Cu(II)Br$_2$/Me$_6$TREN complex to the initiator (0.1 and 0.2). No significant changes were observed in the MW control, since both PDPA present similar low MW tailing (Fig.S3- ESI†).

Influence of different ATRP initiators on the rate of polymerization and control over molar mass of DPA in IPA/water mixtures

In order to evaluate the possibility of preparing telechelic PDPA with different chain-end functionalities, an alkyne terminated initiator (PgBib) was used in the SARA ATRP reactions of DPA. Fig. 5 presents the kinetic plots of DPA polymerization for a DP of 40.

When PgBiB was used as ATRP initiator (Fig. 5) the kinetic plot showed similar behavior compared to EBiB. The polymerization reaches high monomer conversion (92%) in less than 4 hours

with relatively low dispersity (M$_w$/M$_n$ = 1.22). The kinetic data obtained under the same reaction conditions for normal ATRP revelead a much slower polymerization (Fig. S4).
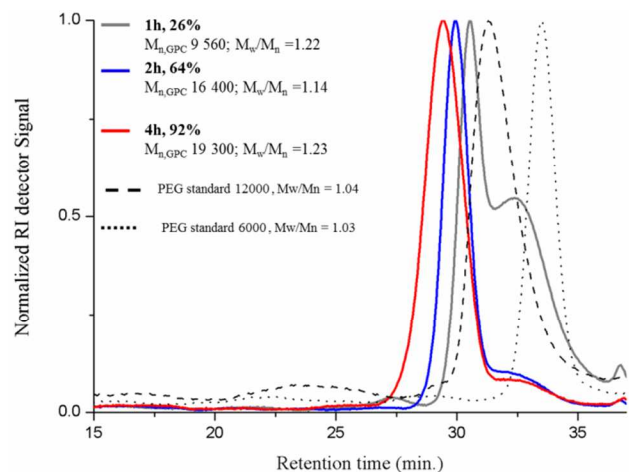

Fig. 6 GPC traces of PEG standard (Mp = 12 000 gmol^{-1}; Mw/Mn = 1.04) and PDPA samples. Conditions: [DPA]$_0$/solvent = 1/2 (v/v), [IPA]/[H$_2$O] = 0.95/0.05 (v/v); [DPA]$_0$ /[PgBiB]$_0$ /[Na$_2$S$_2$O$_4$]$_0$ /[CuBr$_2$]$_0$ /[Me$_6$TREN]$_0$ = 40/1/1/0.1/0.1 (molar); T= 40 ºC.

Additionally, a 4-armed ATRP initiator was further evaluated with this SARA ATRP catalytic system. Star-shaped initiators can generate complex polymeric architectures, which may provide unique functionalities in biomedical applications.[33] The use of 4-arms star initiator for the Na$_2$S$_2$O$_4$/Cu(II)Br$_2$/Me$_6$TREN catalytic system in IPA/H$_2$O [95/5 (v/v)] was evaluated to prepare four-armed star PDPA and compare with the linear counterpart. Two polymers with the same total target MW were synthesized using a 4-arms star as initiators and EBiB. The comparison of both GPC traces, from the linear polymer (DP 100) with the 4 arms star polymer with DP 25 (Fig. 7), shows that the trace from the star polymer is eluted at a volume greater than its linear counterpart. In fact, this observation may be explained by the lower hydrodynamic volume that a star polymer occupies when compared to its linear analogue.

For an accurate characterization of the 4-arms start PDPA, the GPC analysis was performed using a multi-detectors systems, including differential viscometer (DV) and a right-angle laser-light scattering (RALLS) detector in addition to the refractive index (RI) detector. Mark-Houwink plots of log intrinsic viscosity as a function of log MW were calculated for the 4-arms star PDPA and the linear analog in order to explore the conformation of the polymer in solution and are presented in Fig.8. The resulting plot of the 4-arms star polymer consists in a parallel line to the linear one indicating that a star polymer has a lower intrinsic viscosity at any given molecular weight when compared to the linear one. The relationship between the MW and the intrinsic viscosity is given by the equation, [η]=k M$^\alpha$, being [η] the intrinsic viscosity, M the molecular weight and k, α the Mark-Houwink constants. The Mark-Houwink exponent (slope of the curves), which depends on the polymer configuration in solution, is considerably lower for the 4-

armsPDPA polymer (*a*= 0.59), indicating a more compact and dense structure, than the linear one (*a*=0.65). The k value

Table 1 SARA-ATRP of PDA in the Presence of $CuBr_2$/Me_6TREN and $Na_2S_2O_4$ at 40 °C in isopropanol/water (monomer/solvent ratio: 1/2 (v/v))

Entry	$[DPA]_0$/[initiator]$_0$/[Na$_2$S$_2$O$_4$]$_0$/ [CuBr$_2$]$_0$/ [Me$_6$TREN]$_0$	Initiator	[IPA]/ [H$_2$O] (v/v)	k_p^{app}(h^{-1})	Time (h) [a]	Conv. (%) [a]	$M_{n,th}^{a}$x10^3	$M_{n,GPC}^{a}$x10^3	M_w/ M_n [a]
1	50/1/1/0.1/0.1	EBiB	0.95/0.05	0.418	5	88	9.55	20.15	1.14
2	50/1/1/0.1/0.1	EBiB	0.90/0.10	0.569	5	83	8.81	20.51	1.66
3	100/1/1/0.1/0.1	EBiB	0.95/0.05	0.416	5	87	18.79	28.14	1.47
4	100/1/1/0.1/0.1	EBiB	0.90/0.10	0.678	5	62	13.35	23.85	1.54
5	20/1/1/0.1/0.1	EBiB	0.95/0.05	---	4	98	4.53	14.32	1.20
6	20/1/1/0.2/0.2	EBiB	0.95/0.05	---	4	92	4.10	15.20	1.20
7	40/1/1/0.1/0.1	PgBiB	0.95/0.05	0.730	5	96	8.01	20.28	1.20
8	100/1/1/0.1/0.1	PgBiB	0.95/0.05	---	14	95	28.76	28.76	1.40
9	90/1/1/0.1/0.1	PgBiB	0.90/0.10	---	2	64	12.42	30.62	1.24
10	100/1/4/0.4/0.4	4-arms star	0.95/0.05	---	5	99	21.69	29.68$^{(*)}$	1.17

[a]Values obtained from the last sample from the kinetic studies. $^{(*)}$ Data from THF GPC.

observed for star and linear polymer was 9.38x10^{-4} and 5.37 x10^{-4}, respectively.

The kinetic data obtained for the different reaction conditions used for the SARA ATRP of DPA are summarized in Table 1. The results indicate that when EBiB was used, as expected, the faster polymerizations were observed for higher contents of water (entries 2 and 4). This observation suggests that high water amount in the system allows faster reduction of Cu(II)Br$_2$ species to Cu(I)Br, which should be related to the higher solubility of the dithionite salt. However, the dispersity obtained is also higher, limiting the content water that can be used in this system to 10% (v/v). It is also interesting to notice that for PgBiB and 4f-BiB imitators (entries 10 and 11) the PDI remains low even using 10%(v/v) of water in the polymerization mixture.

^{1}H NMR and MALDI-TOF-MS analyses

The chemical structure of the PDPA synthesized by SARA ATRP was determined with ^{1}H NMR and MALDI-TOF-MS techniques. A ^{1}H NMR spectrum of a PDPA sample is shown in Fig. 9. The peaks observed at 3.82 ppm (**f**, –OCH$_2$CH$_2$–), 2.98 ppm (**h**, –(CH-N)$_2$–), 2.62 ppm (**g**,–CH$_2$CH$_2$N–), 1.7-2.1 ppm (**d**, –CH$_2$– of the polymer backbone), resonances at 1 ppm (**i**, – (CH(CH$_3$)$_2$-; **e**, "methacrylic" CH$_3$) are in agreement with the expected PDPA chemical structure.[34-37] The peak of the methylene group (**b**) of the initiator fragment (**CH$_2$**) can be found at 4.1 ppm and its three methyl resonances (**a, c**) are overlapped with other methyl group signals at the region around 1 ppm. Although the calculation of $M_{n,NMR}$ for methacrylates is not simple, due to signals overlapping and low intensity of the resonances of the initiator moieties, the degree of polymerization was calculated comparing integrals of **h,** methylene protons at 2.98 ppm and of the sum of **a, c, e,** and **i** methyl protons at 0.9-1.1 ppm. From the ratio $2n/(9+15n) = I_h/I_{a,c,e,i,}$, n = 70 was obtained, the calculated the $M_{n,NMR}$= $M_{initiator}$ + n$M_{monomer}$ = 15,117 which is close to the MW determined by GPC. Comparison of the ^{1}H NMR PDPA spectrum of the PDPA with the ^{1}H NMR spectra of predominantly
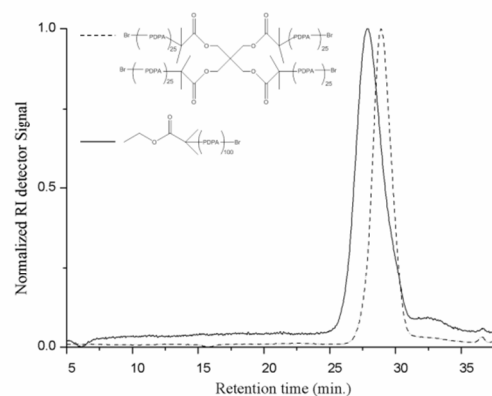

Fig. 7 GPC traces of linear PDPA and 4-arms star PDPA samples. Conditions: $[DPA]_0$/[IPA]/[H$_2$O] = 1/0.95/0.05 (v/v); $[DPA]_0$ /[EBiB]$_0$ /[Na$_2$S$_2$O$_4$]$_0$ /[CuBr$_2$]$_0$ /[Me$_6$TREN]$_0$ = 100/1/1/0.1/0.11 (molar) (linear); $[DPA]_0$ /["4-armed initiator"]$_0$ /[Na$_2$S$_2$O$_4$]$_0$ /[CuBr$_2$]$_0$ /[Me$_6$TREN]$_0$ =100/1/4/0.4/0.41 (star), T= 40ºC.
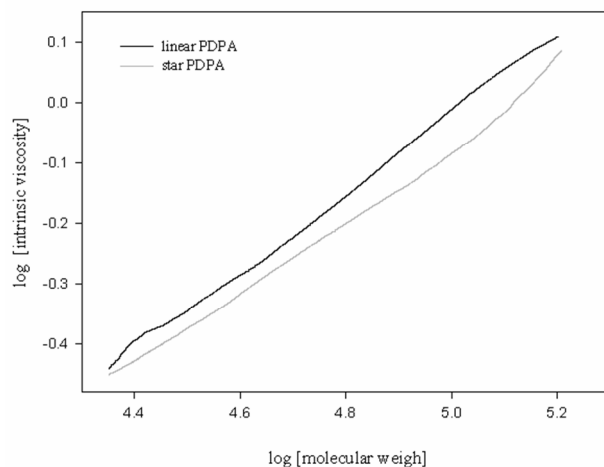

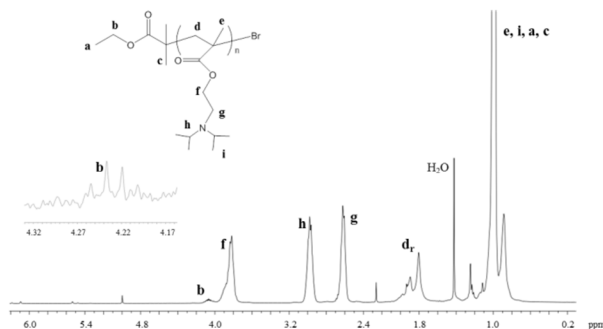**Fig. 8** Log-log plot of intrinsic viscosities against MW for linear and 4-

arms star PDPA.

Fig. 9 The ^{1}H NMR spectrum of PDPA-Br ($M_{n,GPC}$ 14 900 gmol^{-1}; $M_{n,NMR}$ = 15 100 gmol^{-1} M_w/M_n = 1.20) in CDCl$_3$.
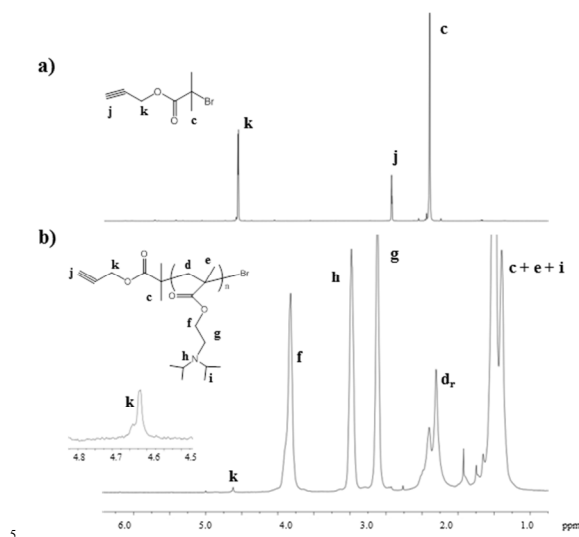

Fig.10 The ^{1}H NMR spectra in CDCl$_3$ of a) PgBib – initiator; b) PDPA-Br obtained at high conversion ($M_{n,GPC}$ 27 900 gmol^{-1}; M_w/M_n = 1.09; $M_{n,NMR}$ = 25800 gmol^{-1}).

syndiotactic poly(methyl methacrylate) (PMMA) (resonances of *racemo* **d$_r$** methylenes at 1.8 ppm) and predominantly isotactic PMMA (two groups of *meso* **d$_m$** methylene signals of the same intensity at 2.4 and 1.4 ppm) [34]) led to conclusion that the PDPA have a very high syndiotactic content due to steric hindrance of the diisopropylaminoethyl moiety. The calculated syndiotactic content is 98% - the ratio of integral values of **d$_r$** (1.7-2.1 ppm) and **h**, methylene protons. This value is in a good agreement with our previous observations of different syndiotacticity for poly(alkyl acrylates) with alkyl groups of different bulkiness (Me, Et, Bu, iBu, tBu, lauryl, 2-Methoxyethyl) obtained by Na$_2$S$_2$O$_4$-catalyzed Single Electron Transfer – Degenerative Chain Transfer Living Radical Polymerization SET-DT LRP.[11, 38-43]

The percentage of the bromo-chain-end functionality cannot be determined since the PDPA signals of the protons near the terminal bromo-chain-end are overlapped with the proton signals of the main polymeric chain (**d, e**).

The presence of chain end functionality for the PDPA synthesized using the PgBiB as ATRP initiator could also be identified by ^{1}H NMR spectroscopy (Fig. 10). In the NMR spectrum of the pure polymer the characteristic peaks of the CH$_3$- and -CH$_2$- groups that are adjacent to the terminal Br chains ends are overlapped with those of the methylene protons of the polymeric chain (**d, e**) and, thus, the degree of active bromo-chain ends could not be calculated. The methylene protons resulting originally from the PgBiB initiator (**k**), which can be observed at 4.62 pm, allows estimating of the number-average MW, $M_{n,NMR}$ = 25800gmol^{-1}.

The MALDI-TOF-MS spectrum of PDPA in the linear mode with m/z ranging from 1400 to 3000 and 1200 to 9500 is shown in Fig.11 and Fig. 12 (a). Enlargement of the latter in m/z 2000-3220 range is shown in Fig. 12 (b). One or two series of main peaks are separated by an interval corresponding to a DPA repeating unit (211 = 213 – 2 = M_{DPA} – M_{H2} mass units), that can be explained by the loss of hydrogen from diisopropylaminoethyl fragment. Tertiary amines are strong photoreducers. [38, 44, 45] Ethyl diisopropyl amine loses hydrogen under photolysis in the presence of a photosenstizer with quantum yield >90% [44]. Under MALDI conditions (excited matrix molecules, laser irradiation) ethyl diisopropyl amine moieties can lose hydrogen quantitatively. It is important to notice that no MALDI-TOF results for PDPA were reported so far.

The assignment of the peaks is presented in Table 2. The general formula for peaks in Fig. 10 and for the bigger set of signals in Fig. 12 (Table 2[a]) is $MW_{MALDI peak n}$ = MWexp = MWca + mH = (EBIB + (DPA-2H)n – Br + K$^+$+ mH), where n – the number of repeat units (DPA-2H), m = (-5) – 5, can depend on MW and MALDI conditions, for example the laser power . Odd values of **m** can indicate that hydrogen abstraction occurs through a radical mechanism that corresponds to literature data. [38, 44, 45] Values of **m** increase with molecular weight. The loss of Br functionality in the polymer structure has been reported in MALDI-TOF MS of acrylate-based polymers produced by ATRP. [46, 47] Thus, the loss of halides could be attributed to the polymerization reactions or a result of fragmentation in the MALDI mass spectroscopy.
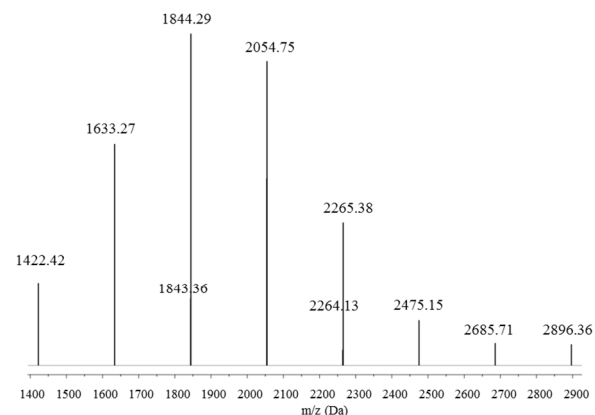

Fig 11: MALDI-TOF-MS in the linear mode (using DHB as matrix) of PDPA-Br ($M_{n,GPC}$ = 14300, M_w/M_n = 1.21) from m/z 1400 to 3000. Conditions: [DPA]$_0$/solvent = 1/2 (v/v), [IPA]/[H$_2$O] = 0.95/0.05 (v/v);

$[DPA]_0/[EBiB]_0/[Na_2S_2O_4]_0/[CuBr_2]_0/[Me_6TREN]_0 = 20/1/1/0.1/0.1$ (molar); T=40ºC.
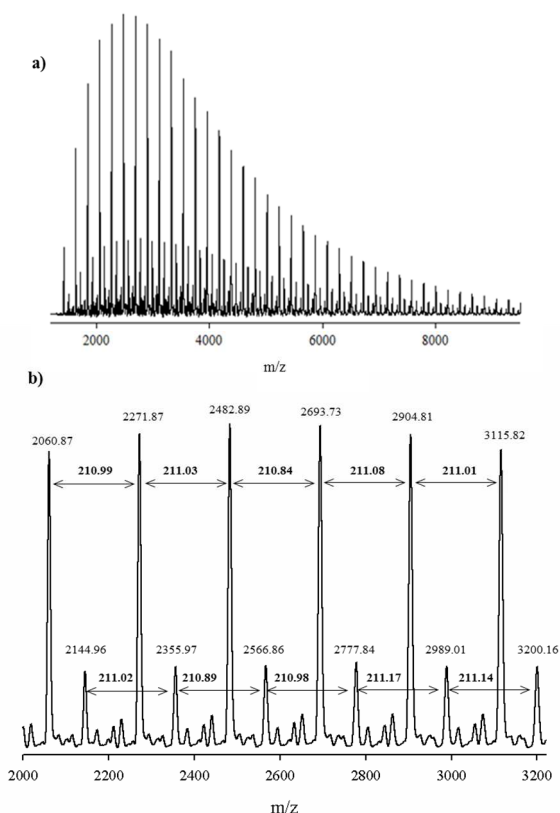

Fig.12 MALDI-TOF-MS (a) in the linear mode (using DHB as matrix) from m/z 1200 to 9500 and (b) enlargement of the MALDI-TOF-MS from m/z 2000 to 3220 of PDPA-Br ($M_{n,GPC}$ = 14300, M_w/M_n = 1.21). Conditions: $[DPA]_0$/solvent = 1/2 (v/v), $[IPA]/[H_2O]$ = 0.95/0.05 (v/v); $[DPA]_0/[EBiB]_0/[Na_2S_2O_4]_0/[CuBr_2]_0/[Me_6TREN]_0$ = 20/1/1/0.1/0.1 (molar); T=40ºC.

The minor peak set in Fig. 12 and Table 2 can be attributed to adduct of the above fragments with 4-hydroxybutanal, $HO(CH_2)_3CHO$, HBA MW 88.11, which in an impurity in THF

solvent.[48] Table 2^b demonstrates an excellent agreement for this suggestion (m = 0; 1).

Chain extension experiment

To prove the presence of the terminal Br chain ends in the growing polymer chains and the "living" nature of the PDPA obtained by SARA ATRP, a chain extension experiment was carried out. As shown in Fig. 13, a shift towards lower retention volumes of the GPC trace of the PDPA sample was observed when new monomer was supplied. The MW of the PDPA macroinitiator obtained at 75% conversion ($M_{n,th}$= 4940 gmol^{-1}, $M_{n,GPC}$ = 15300 g/mol, M_w/M_n = 1.20) nearly doubled, while maintaining a narrow MW distribution, when new monomer was supplied ($M_{n,th}$ = 14400 gmol^{-1} $M_{n,GPC}$ = 27300 g/mol, M_w/M_n = 1.15).
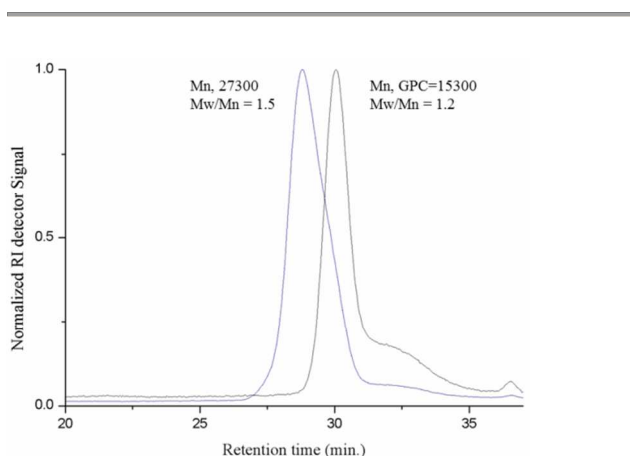

Fig. 13 GPC traces of the PDPA before (black line) and after the chain extension (blue line) experiment.

Table 12: MALDI-TOF MS peaks assignment.

^{a,b}n	^{a}MWca Fig. 10, 12 (major set)	MWexp Fig. 10	^{a}m	^{a}MWexp Fig. 12(major set)	^{a}m	^{b}MWca Fig. 12(minor set)	MWexp Fig. 12(minor set)	^{b}m
6	1422.06	1422.42	0					
7	1633.36	1633.27	0					
8	1844.66	1844.29	0					
9	2055.96	2054.75	-1	2060.87	5	2144.07	2144.96	1
10	2267.26	2265.38	-2	2271.87	5	2355.37	2355.97	1
11	2478.56	2475.15	-3	2482.89	4	2566.67	2566.86	0
12	2689.86	2685.71	-4	2693.73	4	2777.97	2777.84	0
13	2901.16	2896.36	-5	2904.81	4	2989.27	2989.01	0
14	3112.46			3115.82	3	3200.57	3200.16	0

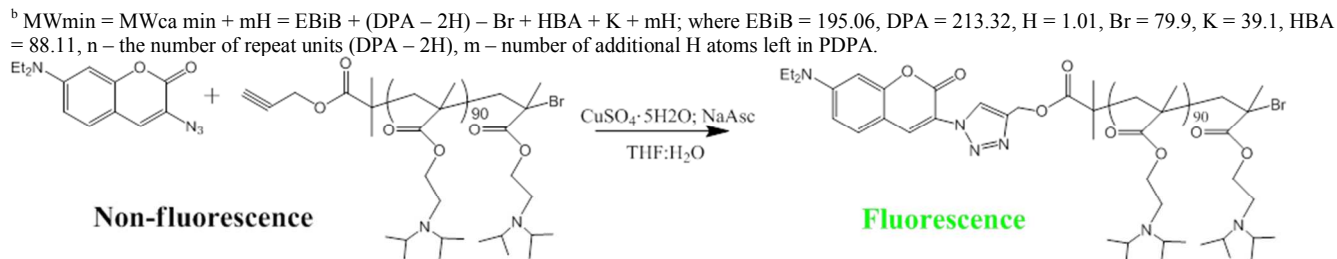^{a} MW = MWca + mH = EBiB + (DPA – 2H) – Br + K + mH;

Fig. 14 "Click" reaction between alkyne functionalized PDPA and 3-azido-7-diethylaminocoumarin.

This result indicates that the "living" character of the synthesized PDPA can be obtained through the application of the $Na_2S_2O_4$-mediated SARA ATRP catalytic system, thus, suggesting that this catalytic system can be applied in the synthesis of block copolymers, with no need of further addition of catalysts to the reaction mixture. Also, the movement toward high MW suggests that the absence of Br functionality observed in the MALDI-TOF part is due fragmentation during the analysis.

N₃-Coumarin reaction with alkyne terminated PDPA

In order to provide further evidence for the presence of the alkyne moiety in the polymer chain end, the AT-PDPA was reacted with an azidocoumarin compound, 3-azido-7-diethylaminocoumarin (Fig. 14). The coumarin dye molecules are biocompatible and have been used as fluorescent molecular probes.[49] Both compounds alone are not fluorescent, but after the azide-alkyne cycloaddition, the formation of the triazole compound provides final structure with fluorescence (highly fluorescent linkage at 366 nm) (Fig. 15).

Fig. 16 presents the NMR spectrum of the "click" reaction product. The characteristic peak of the triazole ring appears at 8.53 ppm (s) and the signal from the methylene protons from the azide chain end functionalized PDPA, which becomes adjacent to the triazol group formed in the "click" reaction, is present at 5.25 ppm (**k**). Moreover, it can be observed that the characteristic peak of the two protons near the alkyne moiety in the AT-PDPA at 4.62 ppm had disappeared, which indicates the complete reaction of the polymer. These results confirms the telechelic structure of the PDPA structures that can be obtained with more environmentally attractive sulphite-base SARA ATRP catalytic system presented in this paper.

Fig. 15 Image of the reaction mixture after the "click" reaction between the alkyne functionalized PDPA and 3-azido-7-diethyl-aminocoumarin. The formation of the fluorescent linkage could be easily seen upon irradiation at 365 nm with a hand-held UV lamp.
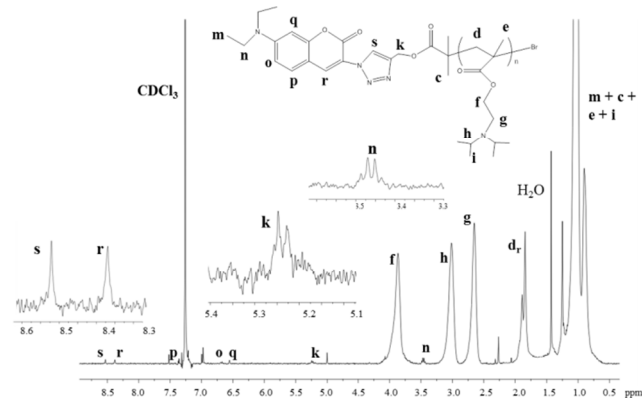

Fig. 16 ^{1}H NMR spectrum, in CDCl₃, of the PDPA-Cu obtained by the "click" reaction between the alkyne-PDPA and the N₃-Cum.

Conclusions

The pH-responsive PDPA was successfully synthesized using an eco-friendly, inexpensive and less toxic SARA ATRP system at 40 °C, in the presence of inorganic sulfites ($Na_2S_2O_4$) and a Cu(II)Br₂/Me₆TREN complex in a mixture of isopropanol and water. The catalytic system was able to control the polymerization of DPA with a low amount of water, 5% (v/v), in the solvent mixture. The controlled/"living" character of this system was supported by kinetic data and chain extension experiments. The controlled molecular structure of the obtained polymers was confirmed by ^{1}H NMR and MALDI-TOF analysis. Moreover, the inclusion of an alkyne chain end functionality was shown to be able to allow post-polymerization functionalization PDPA prepare with this catalytic system through 1,3-dipolar Huisgen cycloaddition.

Acknowledgements

5

Notes and references

^{a} CEMUC, *Department of Chemical Engineering, University of Coimbra, Polo II, Rua Sílvio Lima, 3030-790 Coimbra, Portugal. Fax: +351 239 798 703; Tel:+351 239 798 764; E-mail: jcoelho@eq.uc.pt*

^{b}*Department of Radiology, University of Pennsylvania, Philadelphia, PA19104, United States.*

^{c}*Home Address: 1761 Foster Street, F5B, Philadelphia PA 191116, United States. E-mail: tamazguliasvili@yahoo.com*

^{d}*Department of Chemistry, Carnegie Mellon University, 4400 Fifth Avenue, Pittsburgh, Pennsylvania 15213, United States. E-mail: km3b@andrew.cmu.edu*

20

1 K. Matyjaszewski, *Macromolecules*, 2012, **45**, 4015-4039.

2 W. Jakubowski and K. Matyjaszewski, *Angew. Chem., Int. Ed.*, 2006, **45**, 4482-4486.

3 K. Matyjaszewski, W. Jakubowski, K. Min, W. Tang, J. Y. Huang, W. A. Braunecker and N. V. Tsarevsky, *Proc. Natl. Acad. Sci. U. S. A.*, 2006, **103**, 15309-15314.

4 P. V. Mendonça, A. C. Serra, J. F. J. Coelho, A. V. Popov and T. Guliashvili, *Eur. Polym. J.*, 2011, **47**, 1460-1466.

5 Y. Zhang, Y. Wang and K. Matyjaszewski, *Macromolecules*, 2011, **44**, 683-685.

6 D. Konkolewicz, Y. Wang, M. Zhong, P. Krys, A. A. Isse, A. Gennaro and K. Matyjaszewski, *Macromolecules*, 2013, **46**, 8749-8772.

7 C.-H. Peng, M. Zhong, Y. Wang, Y. Kwak, Y. Zhang, W. Zhu, M. Tonge, J. Buback, S. Park, P. Krys, D. Konkolewicz, A. Gennaro and K. Matyjaszewski, *Macromolecules*, 2013, **46**, 3803-3815.

8 Y. Wang, M. Zhong, W. Zhu, C.-H. Peng, Y. Zhang, D. Konkolewicz, N. Bortolamei, A. A. Isse, A. Gennaro and K. Matyjaszewski, *Macromolecules*, 2013, **46**, 3793-3802.

9 M. Zhong, Y. Wang, P. Krys, D. Konkolewicz and K. Matyjaszewski, *Macromolecules*, 2013, **46**, 3816-3827.

10 C. M. R. Abreu, P. V. Mendonça, A. C. Serra, A. V. Popov, K. Matyjaszewski, T. Guliashvili and J. F. J. Coelho, *ACS Macro Lett*, 2012, **1**, 1308-1311.

11 C. M. R. Abreu, A. C. Serra, A. V. Popov, K. Matyjaszewski, T. Guliashvili and J. F. J. Coelho, *Polym. Chem.*, 2013, **4**, 5629-5636.

12 V. Percec, A. V. Popov, E. Ramirez-Castillo, J. F. J. Coelho and L. A. Hinojosa-Falcon, *J. Polym. Sci., Part A: Polym. Chem.*, 2004, **42**, 6267-6282.

13 Y. H. Ma, Y. Q. Tang, N. C. Billingham, S. P. Armes, A. L. Lewis, A. W. Lloyd and J. P. Salvage, *Macromolecules*, 2003, **36**, 3475-3484.

14 M. Licciardi, Y. Tang, N. C. Billingham and S. P. Armes, *Biomacromolecules*, 2005, **6**, 1085-1096.

15 J. Du, L. Fan and Q. Liu, *Macromolecules*, 2012, **45**, 8275-8283.

16 M. Massignani, I. Canton, N. Patikarnmonthon, N. J. Warren, S. P. Armes, A. L. Lewis and G. Battaglia, *Nature Precedings*, 2010, 4427.

17 F. C. Giacomelli, P. Stepanek, C. Giacomelli, V. Schmidt, E. Jager, A. Jager and K. Ulbrich, *Soft Matter*, 2011, **7**, 9316-9325.

18 K. Zhou, Y. Wang, X. Huang, K. Luby-Phelps, B. D. Sumer and J. Gao, *Angew. Chem., Int. Ed.*, 2011, **50**, 6109-6114.

19 E. J. Lobb, I. Ma, N. C. Billingham, S. P. Armes and A. L. Lewis, *J. Am. Chem. Soc.*, 2001, **123**, 7913-7914.

20 C. Giacomelli, V. Schmidt and R. Borsali, *Langmuir*, 2007, **23**, 6947-6955.

21 K. Liang, G. K. Such, Z. Zhu, Y. Yan, H. Lomas and F. Caruso, *Adv. Mater.*, 2011, **23**, H273-+.

22 A. Blanazs, M. Massignani, G. Battaglia, S. P. Armes and A. J. Ryan, *Advanced Functional Materials*, 2009, **19**, 2906-2914.

23 L. Mueller and K. Matyjaszewski, *Macromol. React. Eng.*, 2010, **4**, 180-185.

24 H. Yu, Y. Zou, Y. Wang, X. Huang, G. Huang, B. D. Sumer, D. A. Boothman and J. Gao, *Acs Nano*, 2011, **5**, 9246-9255.

25 K. Sivakumar, F. Xie, B. M. Cash, S. Long, H. N. Barnhill and Q. Wang, *Org. Lett.*, 2004, **6**, 4603-4606.

26 A. Nadler and C. Schultz, *Angew. Chem., Int. Ed.*, 2013, **52**, 2408-2410.

27 N. Rocha, P. V. Mendonça, J. P. Mendes, P. N. Simões, A. V. Popov, T. Guliashvili, A. C. Serra and J. F. J. Coelho, *Macromol. Chem. Phys.*, 2013, **214**, 76-84.

28 M. Ciampolini and N. Nardi, *Inorg. Chem.*, 1966, **5**, 41-44.

29 J. Z. Du, Y. P. Tang, A. L. Lewis and S. P. Armes, *J. Am. Chem. Soc.*, 2005, **127**, 17982-17983.

30 W. A. Braunecker and K. Matyjaszewski, *Progress in Polymer Science*, 2007, **32**, 93-146.

31 V. Percec, A. V. Popov, E. Ramirez-Castillo, J. F. J. Coelho and L. A. Hinojosa-Falcon, *J. Polym. Sci., Part A: Polym. Chem.*, 2005, **43**, 779-788.

32 S. M. Lough and J. W. McDonald, *Inorg. Chem.*, 1987, **26**, 2024-2027.

33 Y. Zhou, W. Huang, J. Liu, X. Zhu and D. Yan, *Adv. Mater.*, 2010, **22**, 4567-4590.

34 F. A. Bovey, *High Resolution NMR of Macromolecules* Academic Press, 1972.

35 K. Dayananda, M. Kim, B. Kim and D. Lee, *Macromol. Res.*, 2007, **15**, 385-391.

36 C.-L. Peng, L.-Y. Yang, T.-Y. Luo, P.-S. Lai, S.-J. Yang, W.-J. Lin and M.-J. Shieh, *Nanotechnology*, 2010, **21**.

37 F. F. Taktak and V. Butun, *Polymer*, 2010, **51**, 3618-3626.

38 Y. Miyake, K. Nakajima and Y. Nishibayashi, *J. Am. Chem. Soc.*, 2012, **134**, 3338-3341.

39 J. F. J. Coelho, E. Y. Carvalho, D. S. Marques, A. V. Popov, P. M. Goncalves and M. H. Gil, *Macromol. Chem. Phys.*, 2007, **208**, 1218-1227.

40 J. F. J. Coelho, E. Y. Carvalho, D. S. Marques, A. V. Popov, V. Percec and M. H. Gil, *J. Polym. Sci., Part A: Polym. Chem.*, 2008, **46**, 6542-6551.

41 J. F. J. Coelho, E. Y. Carvalho, D. S. Marques, A. V. Popov, V. Percec, P. M. F. O. Gonçalves and M. H. Gil, *J. Polym. Sci., Part A: Polym. Chem.*, 2008, **46**, 421-432.

42 J. F. J. Coelho, J. Gois, A. C. Fonseca, R. A. Carvalho, A. V. Popov, V. Percec and M. H. Gil, *J. Polym. Sci., Part A: Polym. Chem.*, 2009, **47**, 4454-4463.

43 J. F. J. Coelho, A. M. F. P. Silva, A. V. Popov, V. Percec, M. V. Abreu, P. M. O. F. Gonçalves and M. H. Gil, *J. Polym. Sci., Part A:*

Polym. Chem., 2006, **44**, 2809-2825.

44 F. D. Lewis and T.-I. Ho, *J. Am. Chem. Soc.*, 1980, **102**, 1751-1752.

45 S. G. Cohen, A. Parola and G. H. Parsons, *Chem. Rev.*, 1973, **73**, 141-161.

5 46 S. Coca, C. B. Jasieczek, K. L. Beers and K. Matyjaszewski, *J. Polym. Sci., Part A: Polym. Chem.*, 1998, **36**, 1417-1424.
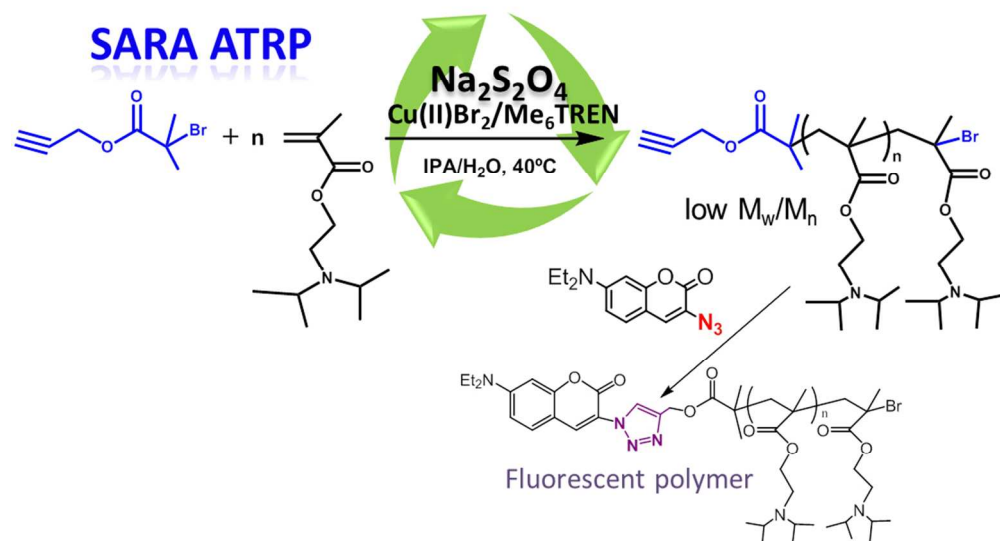
47 D. M. Haddleton, C. Waterson, P. J. Derrick, C. B. Jasieczek and A. J. Shooter, *Chem. Commun.*, 1997, 683-684.

48 X. Lou, C. A. Leenders, A. A. M. Onzen, R. A. Bovee, J. J. Dongen, J. 10 J. M. Vekemans and E. W. Meijer, *J. Am. Soc. Mass Spectrom.*, 2013, 1-4.

49 M.-S. Schiedel, C. A. Briehn and P. Bäuerle, *Angew. Chem., Int. Ed.*, 2001, **40**, 4677-4680.

15

Graphical Abstract
188x105mm (150 x 150 DPI)